Elimination of the friction effects in unconfined compression tests of biomaterials and soft tissues

J Z Wu*, R G Dong and **W P Smutz**
National Institute for Occupational Safety and Health, Morgantown, West Virginia, USA

Abstract: The mechanical properties of biomaterials and soft tissues are determined conventionally using unconfined compression tests. In such tests, frictionless specimen/platen contact in unconfined compression tests has to be assumed in determining the material properties of the materials. Previous theoretical analysis demonstrated, however, that the effects of the friction at the specimen/platen contact interface on the measured stress responses are non-negligible. In this study, a computational approach was proposed to eliminate the effects of friction. The friction coefficient between the specimen and the compression platens is measured first. Using a finite element model, the stress–strain relationship, without the influence of the friction effects, can be derived from the experimental data obtained in conventional unconfined compression tests. In order to validate the proposed approach, unconfined compressive tests of rubber have been performed.

Keywords: compression, finite element analysis, friction, mechanical properties, mechanical test, soft tissue biomechanics

NOTATION

d	diameter of the specimen
D_i $(i = 1, \ldots, N)$	bulk parameters
f	coefficient of friction
h	height of the specimen
J	volumetric ratio
N	number of the terms in the strain energy density function
U	Ogden's strain energy density function
α_i $(i = 1, \ldots, N)$	exponential parameters
ε	nominal (engineering) strain
λ	stretch ratio
λ_i $(i = 1, 2, 3)$	principal stretch ratios
$\bar{\lambda}_i$ $(i = 1, 2, 3)$	deviatoric principal stretches
μ_i $(i = 1, \ldots, N)$	shear parameters
σ	nominal (engineering) stress

1 INTRODUCTION

In unconfined compression tests, the effects of the friction between the specimens and compression platens are traditionally assumed to be negligible, such that the specimens are considered to deform uniaxially and the material parameters can be obtained by fitting the analytical model to the experimental data. However, some previous studies indicated that the effects of the friction on the deformation behaviour of the specimen in unconfined compression were non-negligible. It is well-known that a metallic specimen will barrel at the middle in a uniaxial compression test [**1**], suggesting that the specimen does not actually experience a uniaxial deformation during the test due to the friction effects. Armstrong *et al.* [**2**] and Brown and Singerman [**3**] observed that the peak reaction forces in their unconfined stress–relaxation experiments of articular cartilage exceeded the corresponding maximum values predicted analytically. These authors suggested that this discrepancy might have resulted from the friction between the specimens and the platens. Spilker *et al.* [**4**] analysed the effects of specimen/platen friction on the mechanical response of cartilage in unconfined compression using the finite element (FE) method. Recently, the current authors have analysed the effects of specimen/platen friction on the mechanical behaviour of non-linear soft tissues in unconfined compression tests [**5**]. These theoretical analyses showed that the measured force responses in unconfined compression tests could be overestimated by as much as 50–100 per cent, depending on the dimensions of the specimens, the friction coefficient in the specimen/platen interface and the material properties.

The MS was received on 21 July 2003 and was accepted after revision for publication on 15 October 2003.
** Corresponding author: National Institute for Occupational Safety and Health, 1095 Willowdale Road, Morgantown, WV 26505, USA.*

One common principle to reduce the effects of friction on the experimental results is to minimize the specimen/platen friction during unconfined compressions. For example, Miller and Chinzei [6] covered the moving platen with a polytetrafluoroethylene (PTFE) sheet, while Miller-Young *et al.* [7] used a compression platen of polished stainless steel. However, even in ideally controlled experimental conditions, the friction in the specimen/platen interface in unconfined compression cannot be completely eliminated. Consequently, the mechanical behaviour of biomaterial, as observed via traditional unconfined compression tests, is influenced by the friction between the specimen and the platens.

The compressive stress–strain (σ–ε) relationships of soft tissues obtained using the traditional unconfined compression tests contain the effects of the specimen/platen friction, which cannot be eliminated using any experimental technique. The purpose of the present study was to develop a computational approach to eliminate the effects of the specimen/platen friction on the mechanical behaviour of soft tissues in experimentally obtained data of unconfined compression tests. The proposed approach is based on FE analysis.

2 METHODS

2.1 Unconfined compression test

The unconfined compression tests were performed using a universal micromechanical testing machine (type Mach-I, Biosyntech, Montreal, Canada). The testing machine was equipped with a displacement sensor with a resolution of 0.5 μm and a 98 N (10 kg) load cell with a resolution of 4.50 mN (500 mg). The specimen was unconstrained laterally and was squeezed between two polished stainless steel platens. The bottom platen was fixed, while the upper platen moved downward at a constant speed.

The deformation patterns of the specimen during the deformations were monitored using a microscopic video system, which was composed of a colour CCD camera (JAI, Woburn, Massachusetts, USA) and a microscope video lens (Infinity Photo-Optical Company, Boulder, Colorado, USA). A customized LabView IMAQ Vision program, a PCI-1422 Framegrabber and an AI-16XE-50 DAQCard (National Instruments, Houston, Texas, USA) were used to record the images during the loading. One of the DAQ-Card counters was used to trigger the buffered image acquisition at a rate of 10 Hz.

The cylindrical specimens were made of eraser rubber (NSN 7510-01-317-4222, Skilcraft, San Antonio, Texas, USA), and had a diameter, d, of 6.87 mm and a height, h, of approximately 10 mm. The choice of specimen dimensions was based on the consideration of the loading capacity of the testing machine and the feasibility of observing the deformation patterns. The rubber materials are typically hyperelastic (non-linearly elastic) and nearly incompressible. Theoretically, the proposed approach can be used for any materials, linear or non-linear. Rubber was chosen to validate the proposed approach because it has a non-linear stress–strain behaviour that is typical for many biomaterials and soft tissues.

2.2 Measurement of friction in the specimen/platen interface

The coefficient of friction in the specimen/platen contact interface was measured using custom-made equipment as illustrated in Fig. 1. The rubber specimen was fixed on to a weight block using superglue. The additional weight blocks were added on top of the first weight block to achieve different loading levels. The specimen–weight block was slid on the lower compression platen at a slow speed (approximately 2 mm/s). The compression platen was of stainless steel, it was polished and fixed on to the base plate using double adhesive tape. The sliding force and the normal contact force were measured via the two-dimensional force sensors in the base plate. The friction coefficient is defined as the ratio of the sliding force divided by the normal contact force, when the measured sliding force reaches a steady state. The test were performed using three different weights, which produced three different contact forces of approximately 2, 7 and 12 N. Each measurement was repeated three times. The measured normal contact force was verified using the calibrated weight blocks.

In the uniaxial compression tests, the specimen was considered to be in sliding contact with the platens during the deformation once the test was initiated. Therefore, in the present analysis the sliding friction

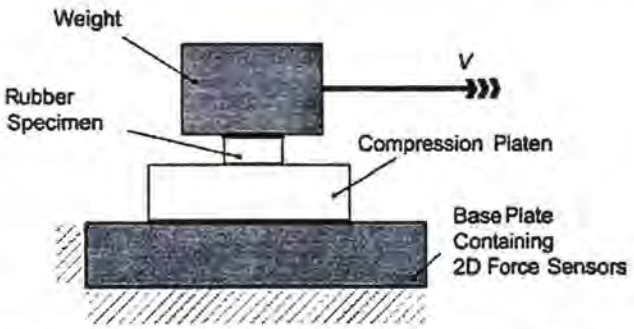

Fig. 1 Schematic of the set-up to determine the friction coefficient of the specimen/platen contact interface. The rubber specimen was fixed on the weight, while the compression platen was fixed on the base plate. The normal contact force was applied via a weight. The weight–specimen block was moved slowly (~2 mm/s), sliding on the compression platen. The contact force and the sliding force were measured simultaneously via the two-dimensional load sensors in the base platen

coefficient, rather than the static friction coefficient, will be used.

2.3 Finite element model

The FE analyses were performed using a commercial finite element software (ABAQUS, version 6.3). The FE model was axisymmetric. The contact between the specimen and the compression platens was modelled using 'contact pair' (an option in ABAQUS) and assuming a constant friction coefficient. The compression platens were specified as 'master' while the specimen was specified as 'slave'.

The steel compression platens were considered to be linearly elastic (Young's modulus, 200 GPa; Poisson's ratio, 0.3). The mechanical behaviour of the rubber specimen was assumed to be non-linearly elastic [**8**], and was modelled using Ogden's [**9**] strain energy function that has been developed for rubber-like non-linear materials

$$U = \sum_{i=1}^{N} \frac{2\mu_i}{\alpha_i^2}[\bar{\lambda}_1^{\alpha_i} + \bar{\lambda}_2^{\alpha_i} + \bar{\lambda}_3^{\alpha_i} - 3] + \sum_{i=1}^{N} \frac{1}{D_i}(J-1)^{2i} \quad (1)$$

where J, the volumetric ratio, $= \lambda_1\lambda_2\lambda_3$, with λ_i $(i = 1, 2, 3)$ being the principal stretch ratios; $\bar{\lambda}_i = J^{-1/3}\lambda_i$ $(i = 1, 2, 3)$ are the deviatoric principal stretches; α_i $(i = 1, \ldots, N)$ are the exponential parameters; μ_i $(i = 1, \ldots, N)$ are the shear parameters; D_i $(i = 1, \ldots, N)$ are the bulk parameters; and N is the number of terms needed to fit to the experimental data satisfactorily.

When the compressibility of the material is neglected, the nominal stress in the stretch direction, λ_u, is obtained from the Ogden strain energy density function in equation (1)

$$\sigma_u = \frac{\partial U}{\partial \lambda_u} = \frac{2}{\lambda_u} \sum_{i=1}^{N} \frac{\mu_i}{\alpha_i}(\lambda_u^{\alpha_i} - \lambda_u^{-\alpha_i/2}) \quad (2)$$

The stretch ratio, λ_u, is related to the nominal strain, ε, by $\varepsilon = \lambda_u - 1$. Owing to the large deformation of the biological materials, the analysis was performed using a finite deformation in the present study [**9**], in which logarithmic strain and Cauchy stress were used in the FE modelling.

2.4 Test procedure

Two tests (referred to as tests A and B) were performed to validate the proposed approach. These two tests were performed using specimens of the same material and dimension ($d = 6.87$ mm; $h = 10.00$ mm), but with different frictional conditions at the specimen/platen contact interface. In test A, the contact interface of specimen and platens was lubricated using liquid soap (Hand Soap, SoftCIDE, Stahmer Weston, Portsmouth, New Hampshire, USA), while it was not lubricated in test B. The unconfined compressive tests were performed at a loading speed of 2 μm/s up to a maximal displacement of approximately 4.00 mm, corresponding to a stretch ratio, λ, of 0.60. It took approximately 33 min for the loading process. Due to the slow loading speed, the viscous effects of the material during the deformation are negligible. The force responses and displacements during the compressive tests were recorded, and the relationship of nominal (engineering) stress–strain of the material was obtained from the experiments. The nominal stress was defined as the force divided by the undeformed cross-sectional area, while the nominal strain was defined as the deformation divided by the undeformed specimen height. Test B was used to calibrate the material parameters, while test A served to validate the obtained 'actual' stress–strain relationship of the material.

The procdure to derive the 'actual' stress–strain relationship consists of four steps: (a) determine the friction coefficient in the contact interface between the specimen and platens; (b) perform the unconfined compression test (test B) to obtain the stress–strain relationship; (c) perform FE simulations to determine the material parameters of the constitutive model using the experimentally obtained stress–strain relationship and friction coefficient; and finally, (d) calculate the 'actual' stress–strain relationship of the material via the constitutive model and the model parameters determined in step (c).

3 RESULTS

The average coefficient of friction, f, between specimen and platens was found to be approximately 0.70 and 0.01 for unlubricated and lubricated contact conditions respectively. The friction coefficient between the rubber specimen and the compression platen was almost independent of the contact force in the force range 2–12 N in which the tests were performed. It was found that the liquid soap was a good lubricant and the friction was negligible in the lubricated specimen/platen contact interface.

In order to check the repeatability of the compressive test results, each loading was run two times and the typical stress–compression-ratio curves are shown in Fig. 2. It can be seen that the difference in the stress–compression-ratio curves obtained in the first and the second run is negligible and the experimental results are highly repeatable.

The effects of friction on the stress responses is demonstrated by comparison of the stress–compression-ratio curve obtained with unlubricated specimen/platen contact (test B) with that with lubricated specimen/platen contact (test A) (Fig. 3). It is seen that, at $\lambda = 0.62$, the stress for the specimen under frictional influence (unlubricated specimen/platen contact) is approximately

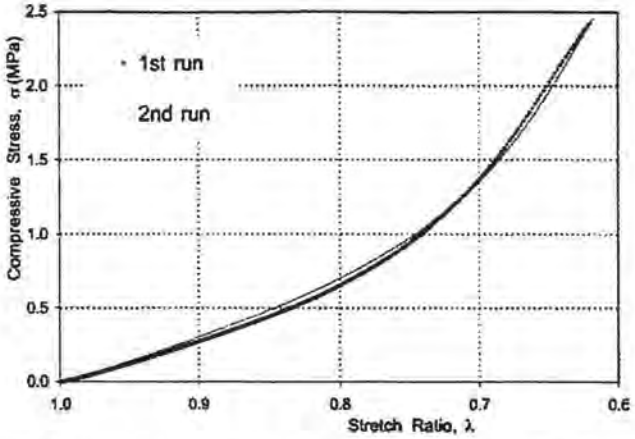

Fig. 2 Stress–compression-ratio curve of the first run compared with that of the second run. The test was performed using the unlubricated specimen/platen contact interface

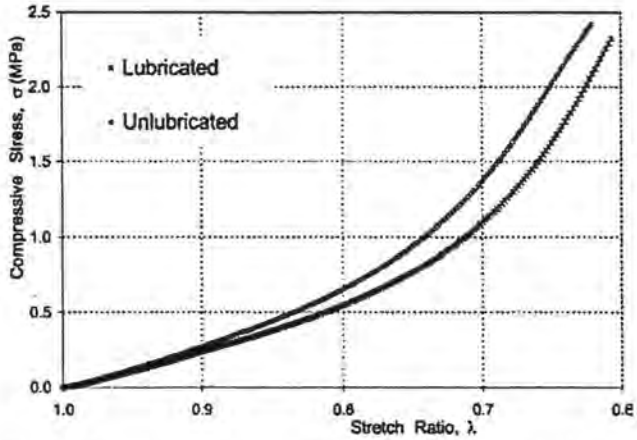

Fig. 3 Stress–compression-ratio curve obtained in the test with the lubricated specimen/platen contact compared with that obtained in the test with unlubricated specimen/platen contact. The difference in these two curves reflects the effects of friction on the stress responses of the specimen

17 per cent higher than that without frictional influence (lubricated specimen/platen contact).

Using the measured friction coefficient for specimen/platen contact ($f = 0.7$) and the stress–compression-ratio relationship obtained for the unlubricated contact, the material parameters for the constitutive model were determined via FE analysis, as listed in Table 1. In ABAQUS and some other commercial FE software packages, the material parameters of the constitutive model can be determined automatically based on the input uniaxial test data. In the FE simulations, the friction coefficient was fixed at 0.7 while the input test data were scaled until the predicted nominal stress–strain curve matched the experimental data. The material compressibility was neglected in the curve-fitting procedure, such that the material parameters could be determined uniquely using the uniaxial test data. It was found

Table 1 Material parameters of the rubber used in the numerical analysis. The parameters were obtained by fitting the FE model to the stress–strain curves of test B (with unlubricated contact)

i	1	2	3
α_i	4.869	6.264	3.494
μ_i (MPa)	−28.136	12.713	15.841
D_i (MPa^{-1})	0	0	0

that a converged solution could be obtained by using a three-term ($N = 3$) Ogden strain energy density function [equation (1)] to fit the experimental data.

The stress–compression-ratio curves calculated using the FE model with the friction coefficient values of 0.7 and 0.0 were compared with those measured with unlubricated and lubricated contact conditions, as shown in Fig. 4. The stress–compression-ratio curve for unlubricated specimen/platen contact was used to calibrate the model parameters, while that for the lubricated specimen/platen contact served to validate the model predictions. The stress–compression-ratio relationship obtained at frictionless specimen/platen contact reflects the 'actual' mechanical behaviour of the material.

Using the same set of material parameters, the stress–compression-ratio relationships of the specimen as a function of specimen/platen friction were predicted via the FE model (Fig. 5). It is seen that the stress level increases with increasing specimen/platen friction. However, the stress–compression-ratio curve varies little and tends to converge to a steady state as the value of the friction coefficient, f, increases to values over 0.4.

In order to facilitate comparison of the theoretical predictions with experimental data, the results presented in Figs 4 and 5 are based on the nominal (engineering) stress and stretch ratios, which are defined as the force

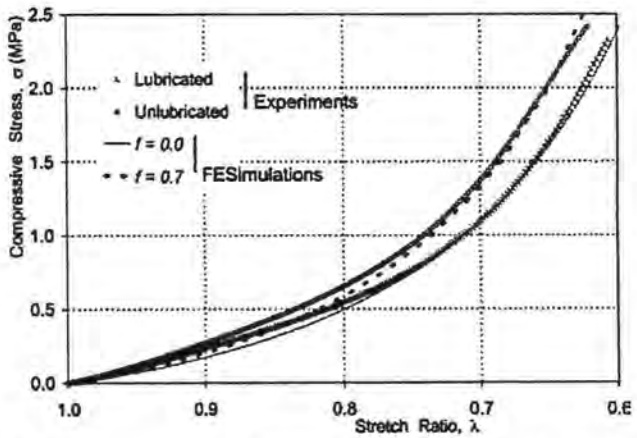

Fig. 4 Comparison of the stress–compression-ratio curves obtained using the FE model (assuming the friction coefficient, f, to be 0.0 and 0.7) with those obtained in the unconfined compression tests (with lubricated and unlubricated specimen/platen contact)

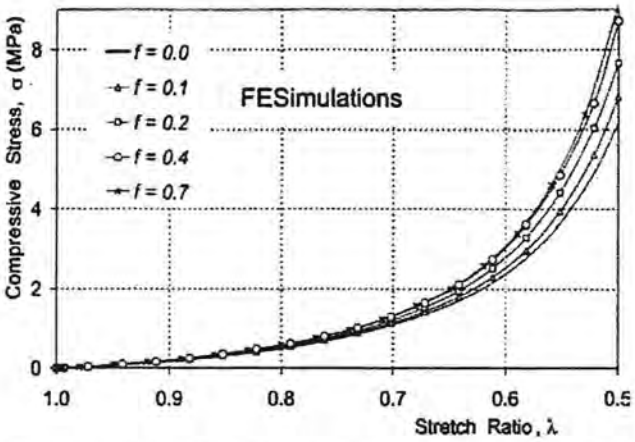

Fig. 5 Predicted stress–compression-ratio relationships as a function of the friction coefficient, f. The stress responses of the specimen increase with increasing friction coefficient. The predicted stress–strain relationship of the material varies little and tends to reach a steady state when f increases to values over 0.4

divided by the undeformed cross-sectional area and the deformed specimen height divided by the undeformed specimen height respectively. The forces were either measured experimentally or calculated using the FE model.

The deformation patterns of the specimen without lubrication were compared with those with lubrication (Fig. 6). It is seen that the deformed specimen barrelled at the middle under large deformation when the specimen/platen contact interface was not lubricated (Fig. 6a), while it did not barrel when the specimen/platen contact interface was lubricated using liquid soap

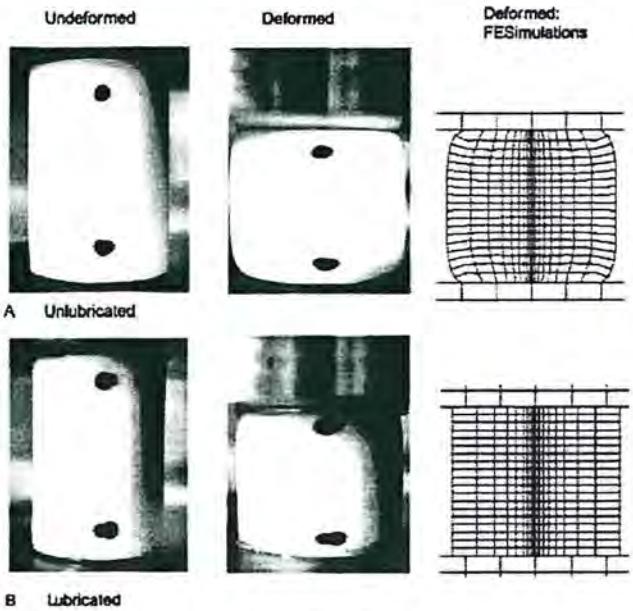

Fig. 6 Deformation patterns of the specimen in the unconfined compression tests. (a) Unlubricated specimen/platen contact. (b) Lubricated specimen/platen contact. $\lambda = 0.65$ at the deformed state

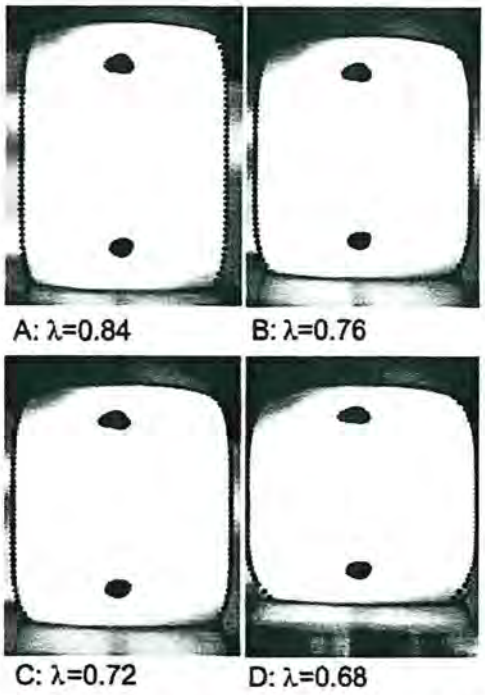

Fig. 7 Deformation patterns of the specimen in the unconfined tests with the unlubricated specimen/platen contact; FE predictions versus experimental observations. The dots represent the predicted lateral outlines of the deformed specimen using the FE model. The friction coefficient was assumed to be 0.7 in the FE simulations

(Fig. 6b). The ends of the specimen cannot be viewed clearly in the photograph (Fig. 6b) due to the excessive lubricant (liquid soap). However, if the regions close to the specimen ends are ignored, the lateral outline of the specimen seems nearly straight.

The deformation-dependent shape variations of the specimen without lubrication, that were predicted using FE model, are compared with those obtained experimentally (Fig. 7). The figure shows that the predicted specimen deformation patterns agree well with the experimental observations, suggesting that the assumption of material incompressibility is appropriate for rubber. The slight difference between the predicted outline and the experimental observation at the bottom end of the specimen (Fig. 7d) was due to the imperfection of the specimen preparation.

4 DISCUSSION AND CONCLUSION

In unconfined compression tests, the friction between the specimen and platens is known to influence the measured force responses [4, 5]. The effects of friction on the force–stress response of biological materials in unconfined compression tests cannot be eliminated experimentally. Consequently, the published data on the compressive behaviour of soft tissues probably contain friction-induced errors of unknown magnitude. Using the proposed approach, the effect of friction on the

measured stress responses in unconfined compression tests can be eliminated.

In the present analysis, the stress–compression-ratio curve for $f = 0.7$, obtained using an FE model, were fitted to the experimental data, such that the material parameters could be determined. The predicted stress–compression-ratio curve for $f = 0.0$, which reflects the mechanical behaviour of the specimen without the frictional influence, agrees well with the experimental stress–compression-ratio curve for the test with a lubricated specimen/platen contact interface, which served to validate the proposed approach. According to the test results, the friction is negligible in the lubricated specimen/platen contact interface; such that, in the unconfined compression tests with the lubricated specimen/platen interface, the specimen was compressed, approximately, in a uniaxial stress state (Fig. 6).

In the example presented in the current study (Fig. 5), it was demonstrated that the measured stress responses obtained in the conventional unconfined compressive tests are greater than the 'actual' stress by as much as 50 per cent at $\lambda = 0.5$. The effects of friction increase dramatically with decreasing stretch ratio. Soft tissues usually undergo very large deformation at physiological loading conditions. Therefore, the specimens of soft tissues have to be loaded up to large deformations in the unconfined compressive tests to mimic these physiological loading conditions. Consequently, stress values could be greatly overestimated in conventional unconfined compression tests.

In this study, the friction coefficient between the rubber specimen and the polished stainless steel platen was determined to be approximately 0.7. It was found that the friction coefficient could not be reduced by refining the smoothness of the compression platens. The reason for this phenomenon may be that the friction here is mainly due to the adherence of the contacting surfaces when a smooth metallic platen is in contact with a relatively softer specimen. In such a case, the only effective approach to reduce the adherence friction is to apply a suitable lubricant. However, the specimen/platen contact surface cannot be lubricated for most tests. This is because (a) the mechanical properties of biological materials could be changed by the lubricant and (b) the friction in the specimen/platen contact interface is needed to hold the specimen in place during the compression. Therefore, it is impossible to eliminate specimen/platen friction in unconfined compression tests of soft tissues.

Previous theoretical analysis [5] suggested that the specimen aspect ratio, d/h, greatly influences the frictional effect on the stress response of the samples. In the present study, however, only one particular specimen dimension was used to demonstrate the application of the proposed technique. This approach can be used for any axisymmetric specimens of any materials, as long as the specimens do not buckle during the compressive loading.

The current analysis (Fig. 5) demonstrated that the effects of the specimen/platen friction reached a 'saturate' state when the friction coefficient reaches a certain value, indicating that there is little relative sliding between the specimen and the compression platen. Most biological materials tend to adhere to the compression platens in unconfined compression tests. Therefore, it is in most cases unnecessary to have an accurate value of the friction coefficient in the specimen/platen contact interface for FE simulations.

In summary, in this study an approach was proposed to obtain the 'actual' stress–strain relationship of soft tissues from the experimental stress–strain curves in unconfined compression tests. The proposed approach made it possible, for the first time, to study the deformation behaviours of biological materials that are not under the influence of the specimen/platen friction, via unconfined compression tests.

ACKNOWLEDGEMENTS

The authors would like to thank Mr C. Warren, Mr D. Welcome for their help in conducting the friction test, and Ms A. Brumfield for setting up the microscopic video system for the material testing.

REFERENCES

1 **Hibbeler, R. C.** *Mechanics of Materials*, 5th edition, 2002 (Prentice Hall, Englewood Cliffs, New Jersey).
2 **Armstrong, C. G., Lai, W. M.** and **Mow, V. C.** An analysis of the unconfined compression of articular cartilage. *J. Biomech. Engng*, 1984, **106**(2), 165–173.
3 **Brown, T. D.** and **Singerman, R. J.** Experimental determination of the linear biphasic constitutive coefficients of human fetal proximal femoral chondroepiphysis. *J. Biomechanics*, 1986, **19**(8), 597–605.
4 **Spilker, R. L., Suh, J. K.** and **Mow, V. C.** Effects of friction on the unconfined compressive response of articular cartilage: a finite element analysis. *J. Biomech. Engng*, 1990, **112**(2), 138–146.
5 **Wu, J. Z., Dong, R. G.** and **Schopper, A. W.** Analysis of effects of friction on the deformation behavior of soft tissues in unconfined compression tests. *J. Biomechanics*, 2004, **37**(1), 147–155.
6 **Miller, K.** and **Chinzei, K.** Constitutive modelling of brain tissue: experiment and theory. *J. Biomechanics*, 1997, **30**(11–12), 1115–1121.
7 **Miller-Young, J., Duncan, N.** and **Baroud, G.** Material properties of the human calcaneal fat pad in compression: experiment and theory. *J. Biomechanics*, 2002, **35**(12), 1523–1532.
8 **Wu, J. Z., Dong, R. G.** and **Smutz, W. P.** Nonlinear and viscoelastic characteristics of skin under compression: experiment and analysis. *Biomed. Mater. Engng*, 2003, **13**(4), 373–385.
9 **Ogden, R.** *Non-linear Elastic Deformation*, 1997 (Dover Publications, Inc., Mineola, New York).